Journal of Seismology **4:** 297–319, 2000.

Stress Field in Costa Rica, Central America

Ronnie Quintero[1,2] & Federico Güendel[1,2]
[1]*Observatorio Vulcanologico y Sismologico de la Universidad Nacional de Costa Rica (e-mail: rq@geofys.uu.se)*
[2]*Department of Earth Sciences, Seismology, Uppsala University (e-mail: fgu@geofys.uu.se)*

Received 4 December 1998; accepted in revised form 7 September 1999

Key words: fault plane, polarities, relocation, stress

Abstract

We have relocated 1658 earthquakes which occurred in Costa Rica, and its vicinity. These relocated earthquakes were then used to investigate the stress and orientation of fault planes within the study area. The analysis was made using the polarities of first motion P-waves. We found that the subduction zone for Costa Rica is mainly characterized by thrust faulting, with some areas also exhibiting a component of strike-slip motion. The intraplate Caribbean seismicity in central Costa Rica shows a predominant shallow left-lateral strike-slip faulting. In southern Costa Rica, the subduction of very young oceanic lithosphere beneath the Caribbean plate (i.e. Panama Block), enhanced by the collision and subduction of the Cocos Ridge, has produced a highly compressive stress regime. This highly compressive regime is characterized by strike-slip faults oriented in a NE-SW direction, extending all the way from the Pacific margin into the back-arc, connecting with the North Panama Deformed Belt.

Introduction

Since 1984, the Observatorio Vulcanologico y Sismologico de Costa Rica, Universidad Nacional (OVSICORI-UNA) has operated a seismographic network (Güendel et al., 1989). Earthquake locations in Costa Rica and surrounding areas have greatly improved with the installation of this and others local seismic networks. This improvement has provided new levels of resolution capable of allowing researchers to revise and propose new tectonic models.

One of these propositions is that Costa Rica is a seismotectonic active zone, where one of the main tectonic features corresponds to the subduction of the Cocos plate beneath the Caribbean plate. Therefore, the interplate seismicity is mainly associated with this tectonic feature and the earthquake hypocenters reach a maximum depth between 200–300 km (see Protti et al., 1995). On the other hand, the intraplate Caribbean and Panama Block seismicity is very shallow. Central America is tectonically and geologically complex and its main tectonic characteristics (e.g. volcanic chain, subduction zones, seamounts, shear and fractures zones) are the result of the interaction of five major lithospheric plates, specifically the North America, Caribbean, Cocos, Nazca and South American plates (see Figure 1).

The convergence rate between the Cocos plate and the Caribbean plate offshore Costa Rica increases from 87 mm/yr in the North to 92–95 mm/yr in the south. The direction of convergence is about N25°-30°E (Minster and Jordan, 1978; De Mets et al., 1990).

The purpose of this study is to investigate the stress tensor distribution for the region of Costa Rica. The investigation is made for different zones in which we divided the region. In this study, first we made a joint inversion of the selected events. We then use the earthquake location and tectonic information from the region to choose different zones, where the stress analysis is made. Finally, we examined the results for different input velocity models and earthquake locations.

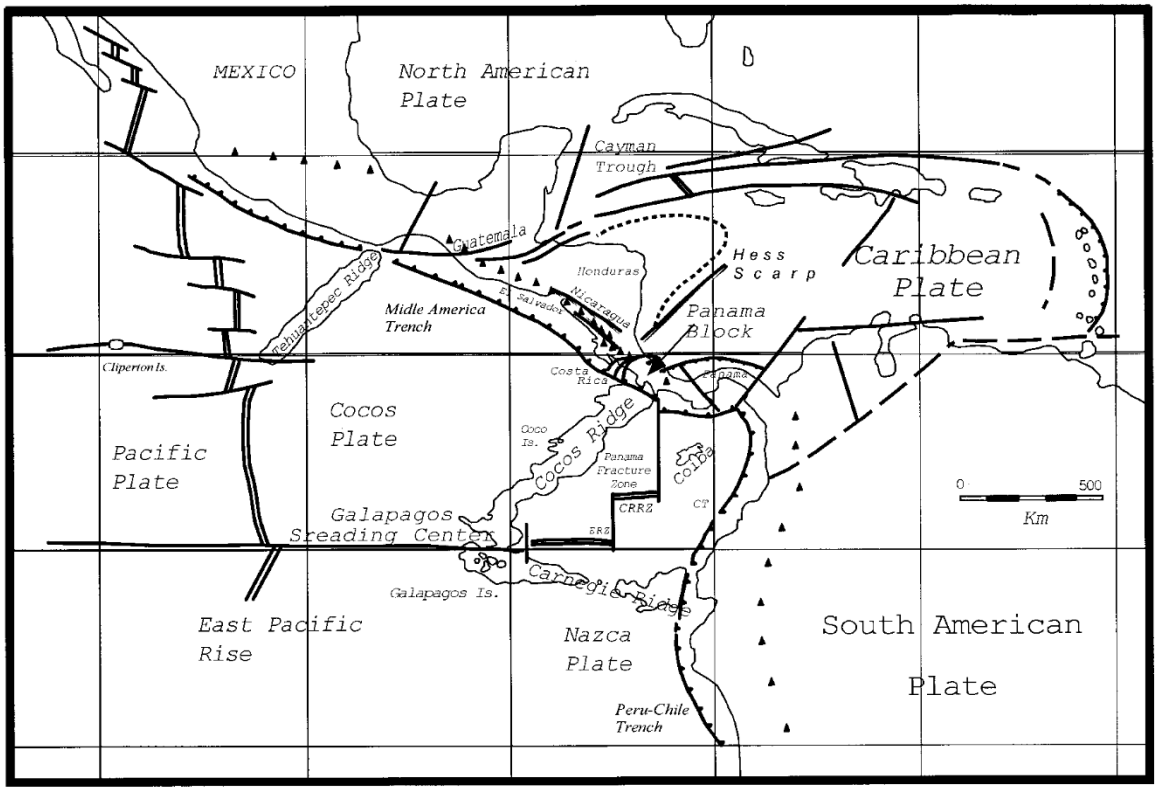

Figure 1. Tectonic setting of Central America, where the major tectonic plates and active volcanoes (indicated by triangles) are shown. Thick lines along central Costa Rica represent the shear zones that mark the boundary between the Caribbean plate and Panama Block. ERZ: Ecuador Rift Zone; CRRZ: Costa Rica Rift Zone; CT: Colombia Trench. ‖ Spreading Axis; — Transform Fault; ▲ Subduction Zone; ⊨ Normal Faults.

Data and method

The data set used in this work is confined to the area 7°-12°N latitude and 82°-88°W longitude, and a depth range of 0–250 km and comprises events occurring during the period of 1984–1997. The data set used has been mainly collected by OVSICORI-UNA seismographic network. This seismographic network of 23 stations, recorded in analog format on paper between 1984 and 1991, thereafter a parallel digital recording system (50 Hz sampling rate) has been operating. Seismometers are mainly short period vertical-component Rangers model SS-1 (1 Hz). The principal data gathered by the network, are P and S wave arrival times from local and regional earthquakes, polarities and coda duration. Data is transmitted from field stations to the recording center using high frequency radio waves (VHF and UHF). Some of the stations used in this study have been deployed on a temporarily basis. Figure 2 shows the location of seismic stations used in this study.

The initial procedure was to utilize the reported epicenters or initial locations of recorded events as shown in Figure 3. These events were located using Hypoinverse program after Klein (1984) and a modified crustal model (Matumoto et al., 1977; model MM in Table 1). From a total of 23979 earthquakes, we selected events with a) 14 or more readings; b) at least 10 P-wave polarities; c) epicentral and focal errors less than 3 and 5 km, respectively; d) local coda magnitude Mc≥2.1. After applying those initial conditions our data set was reduced to 1658 events.

Using the selected events, we performed a Joint-Hypocenter-Determination (JHD). For relocation, we used A1 model (see Table 1); the S-wave velocity was fixed by assuming a P-to-S wave velocity ratio of 1.78. This procedure was carried out using the program VELEST (Kissling et al., 1994). VELEST uses P- and S-arrival times data in a damped least squares inversion procedure to simultaneously estimate, hypocenters, station delays, and velocities in a horizontally layered model (Crosson, 1976); for fixed velocity

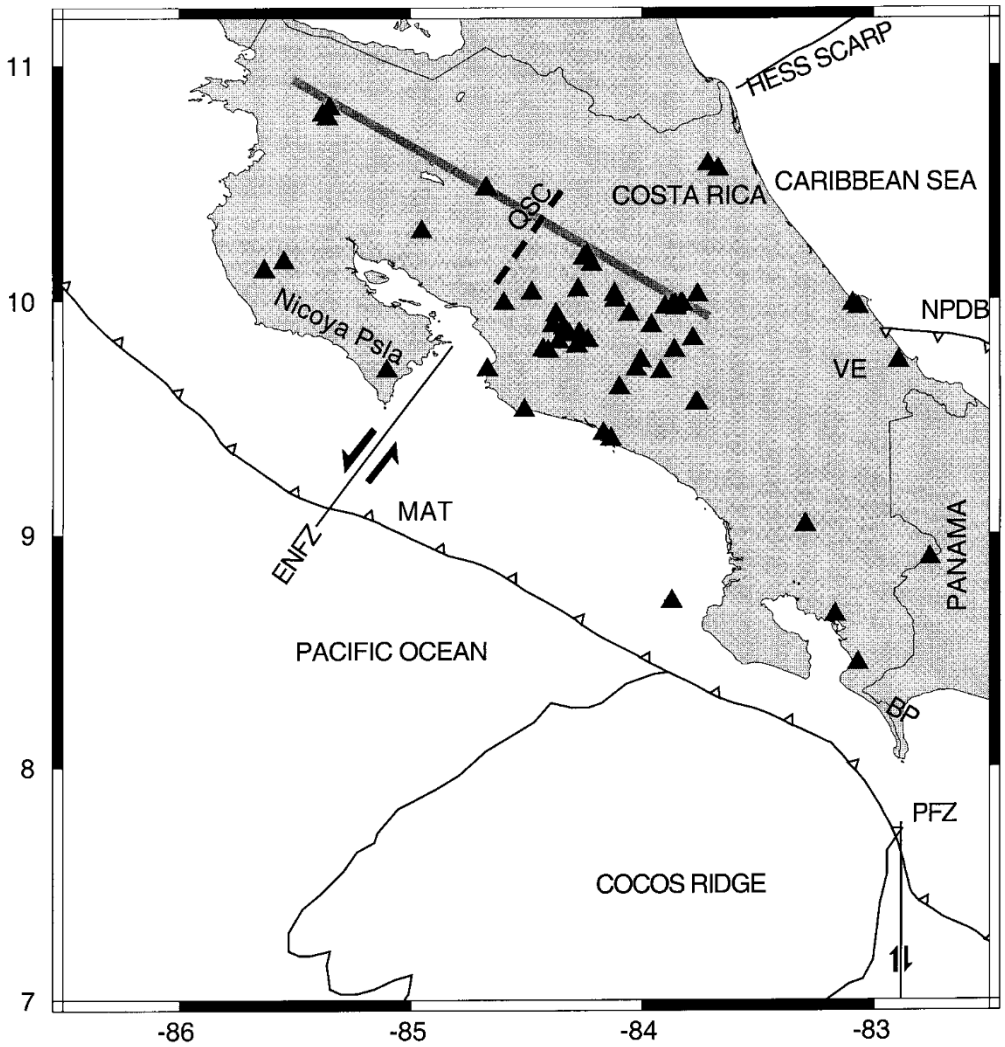

Figure 2. Distribution of seismographic stations (solid triangles) used in this study. A gray line indicates the volcanic arc. MAT refers to Middle America trench, PFZ to Panama Fracture Zone, ENFZ to East Nicoya Fault Zone, BP to Burica Peninsula, Nicoya Psla to Nicoya Peninsula, VE to Valle de la Estrella, NPDB to North Panama Deformed Belt and QSC to Quesada Sharp Contortion.

model and station corrections it performs the JHD (Kissling, 1994). The used P-wave velocity model A1, is a modified crustal model after Matumoto et al. (1997), incorporating information of Protti et al. (1996), and Quintero and Kulhanek (1998). The last authors used Wadati diagrams and concluded that the ratio Vp/Vs = 1.78 is reliable for the study region. We believe that further investigation is necessary, especially using three component seismic station data, but OVSICORI-UNA seismic stations are mainly vertical component. The new locations obtained using this technique are called relocated events.

Hypocenter output of the JHD and model A1 were then used to compute takeoff angles and azimuths for each source-station pair, process attained with the computer program AZTAK (Suetsugu, 1995). Hypocenter parameter, with station polarity information, i.e. station name, azimuth, takeoff angle and polarity (compression or dilatation) were then saved on a polarity data file.

To estimate the principal-stress orientation, the relative stress magnitudes and the orientation of fault planes, we applied the inverse algorithm of Horiuchi et al. (1995). This inverse algorithm is used to find four of the six independent components of the stress

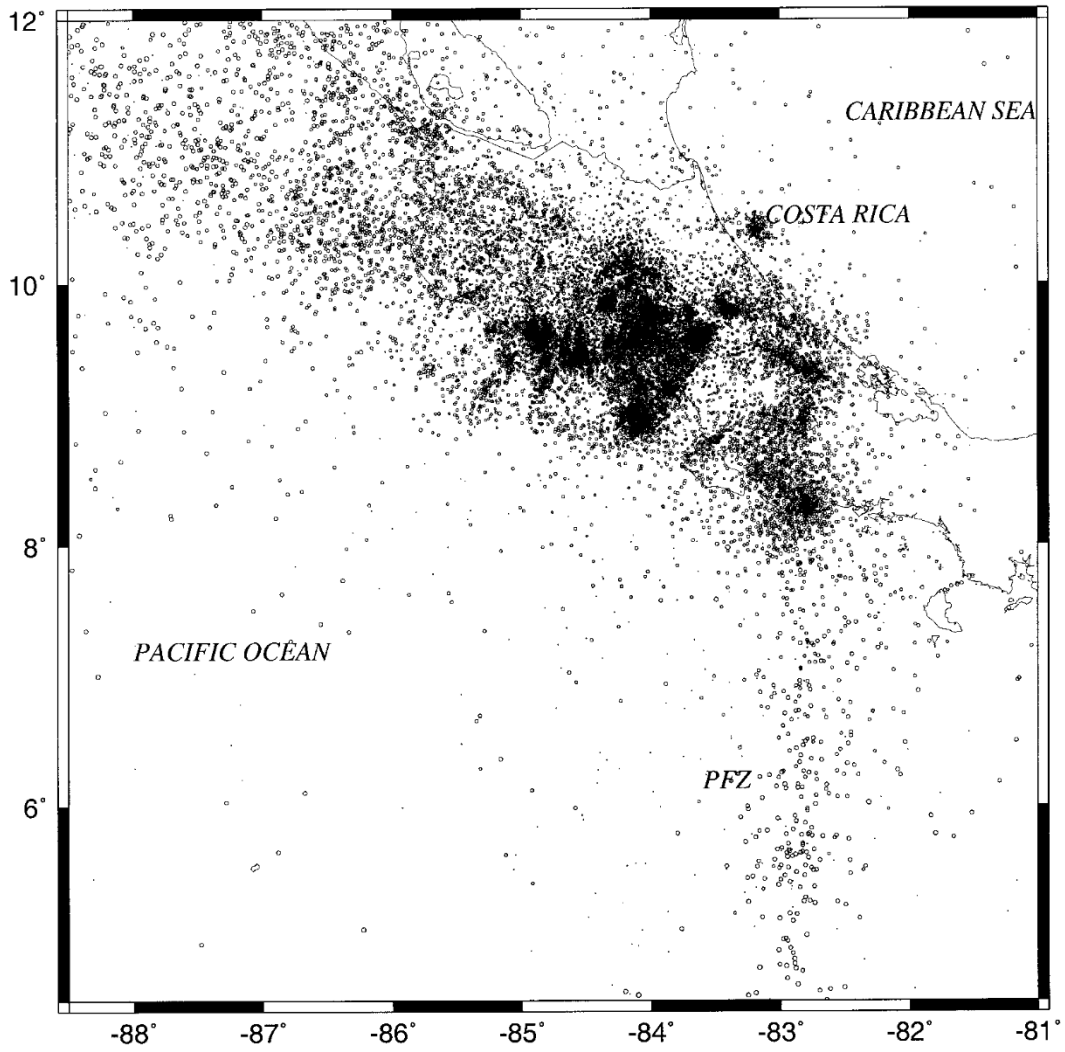

Figure 3. Earthquake epicenter distribution of OVSICORI data set.

tensor: the maximum σ_1; intermediate σ_2; and minimum stresses σ_3; as well as the shape factor R of the deviatoric stress. It is considered that $\sigma_1>\sigma_2>\sigma_3$, and $R = (\sigma_1-\sigma_2)/(\sigma_1-\sigma_3)$; the hydrostatic term is neglected by allowing $\sigma_1+\sigma_2+\sigma_3 = 0$. The R-value is a scalar quantity describing the relative stress magnitudes (Cisternas, 1985). The algorithm simultaneously determines parameters of the stress tensor and the orientation of fault planes, by using readings of P wave polarity. It is further assumed that: a) the stress is uniform for the whole data set; b) earthquakes occur along weak planes with orientation randomly distributed; c) the slip direction of the faulting is parallel to a direction where the shear stress is maximum (Horiuchi et al., 1995). The data set is not required to have the same focal mechanism solution; they are related by compatibility with the stress tensor of the area (i.e. they may have different fault planes).

In the stress tensor inversion, we use data with at the most one inconsistent polarity for the best-fit focal mechanism solution of individual events. It is assumed a double couple model at the source. We emphasized that best focal mechanism solution calculated in this step is not used in the determination of the principal stress.

Using the calculated parameter of the stress tensor, we then estimate permissible ranges of fault plane orientation for each event. The estimation is made by calculating the number of inconsistent stations for all values of strike and dip angles of the fault planes using

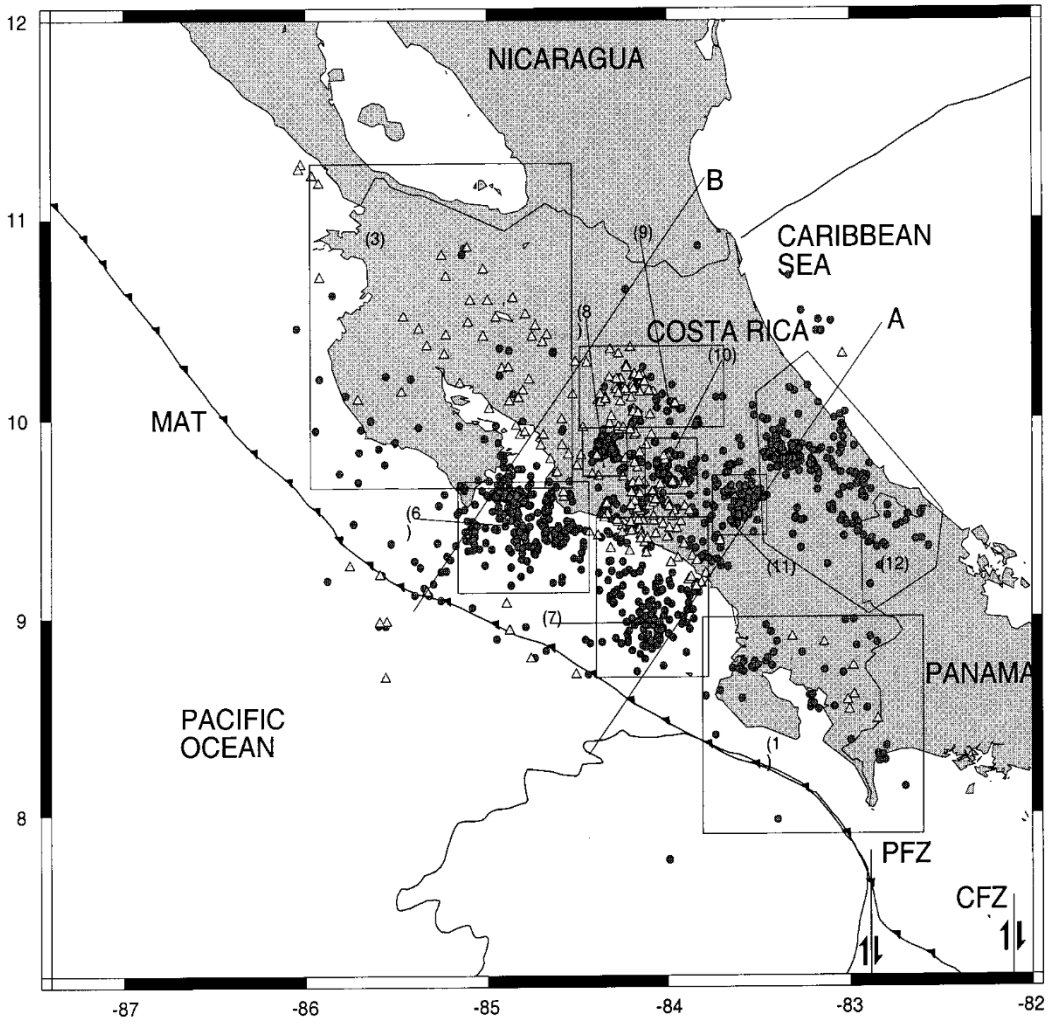

Figure 4. Earthquake epicenter distribution. Circles show the entire data set of 1658 relocated events relocated by joint hypocenter inversion. The figure also shows the twelve selected zones. These regions are denoted by numeral between (1) to (12). Line A and B are the separation for the southern, central and northern subduction zones. CFZ refers to Coiba Fracture Zone.

a grid spacing of 5°. Fault planes having the minimum number of inconsistent stations are finally selected.

Results

Relocation

Earthquakes epicenter of the 1658 relocated events are shown in Figure 4. These events are grouped into two categories according to their focal depth, circles and triangles show the earthquake epicenter depth distribution of these events, corresponding to 0–35 km and 35–250 km, respectively. The resulting epicenter distributions of relocated events do not differ distinctively when compared to the initial earthquake locations. The new hypocenters are slightly shallower than their corresponding initial locations, and the total RMS was reduced to 51% compared with initial locations. Cross section of Figure 5 shows the change in hypocenter location, before and after JHD of events. Similar major tectonic structures compared with previous results for the region (see Protti et al., 1995) can be derived from hypocenter of relocated events. Specifically, the subduction of the Cocos plate beneath the Caribbean plate. The subduction zone of Costa Rica can be divided into 3 different segments: northern, central and

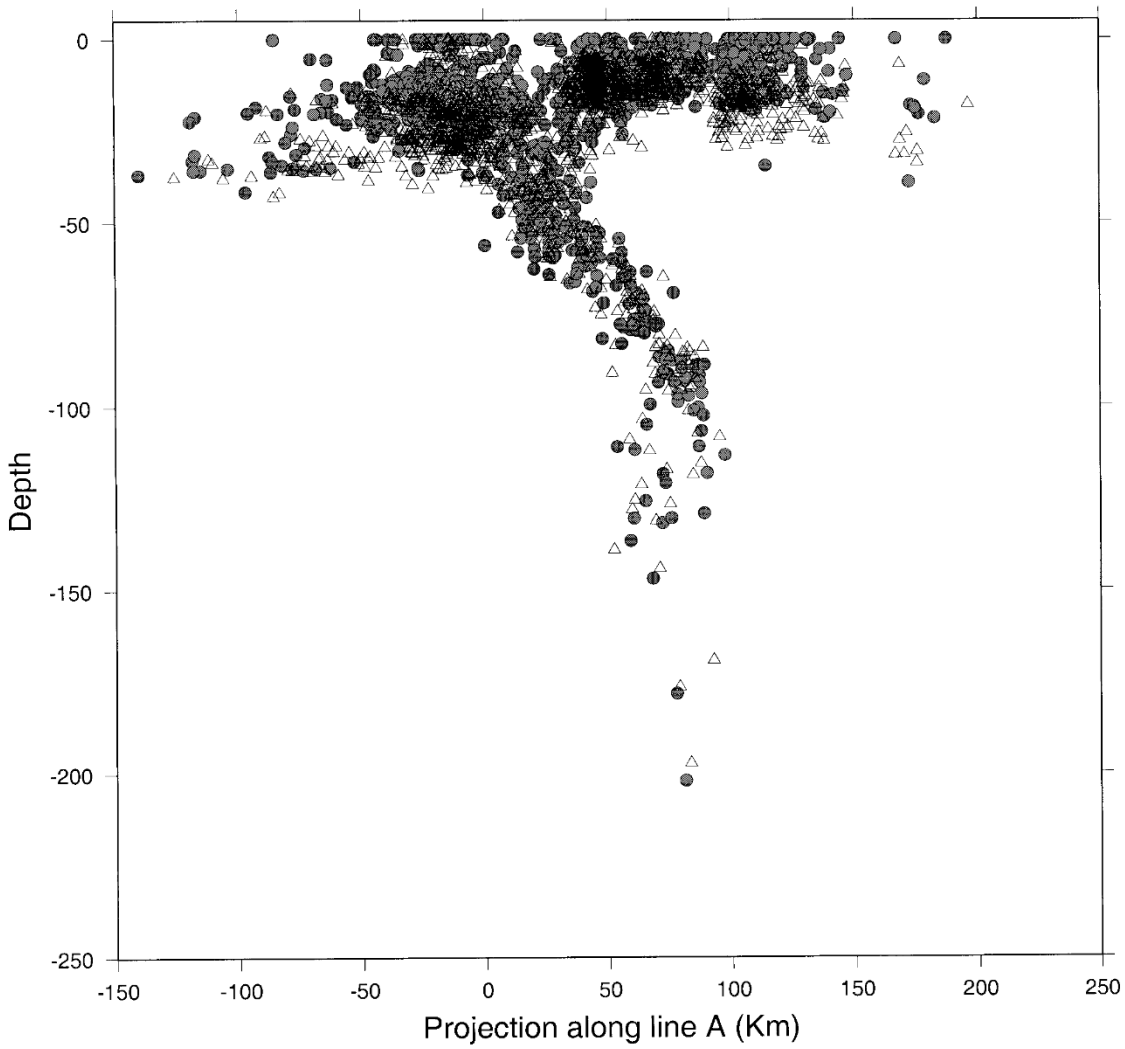

Figure 5. Cross-section of the seismicity before relocation (triangles) and after relocation (circles) projected along line A. The reference point is 9.03° N and 83.9° W.

southern (see Figure 6). The ages of the Cocos oceanic lithosphere subducting beneath the Nicoya Peninsula in northern Costa Rica, is older than that being subducted beneath central and southern Costa Rica was calculated to be 25–30, 20–22 and 13–17 m.y. at trench, respectively (Protti et al., 1995).

A noticeable epicenter alignment, off the Pacific coast, is indicated by line B on Figure 4. This anomaly is associated with the Fisher seamount, which is subducting below the Caribbean plate and marking the separation between irregular and flat seafloor (Hey, 1977; Von Huene et al., 1995). To the northwest of this boundary, the seafloor of the Cocos plate, seaward from the MAT in northern Costa Rica, has a flat morphology (Von Huene et al., 1995). The projection of this alignment into the continental slope is known as the East Nicoya Fracture Zone (ENFZ) (see Figure 2). The further projection of this line along the subducted slab marks the boundary that separates the northern segment from the central segment and known as the Quesada Sharp Contortion (QSC) (Protti, 1991; Protti et al., 1995) (see also Figure 2). To the southeast of this boundary (line B) we find the seamount domain including the Cocos Ridge. From the epicentral distribution we can observe that few events with depths greater than 35 km occur in south-eastern Costa Rica and probably associated to the subduction of a very young oceanic crust. This depth anomaly

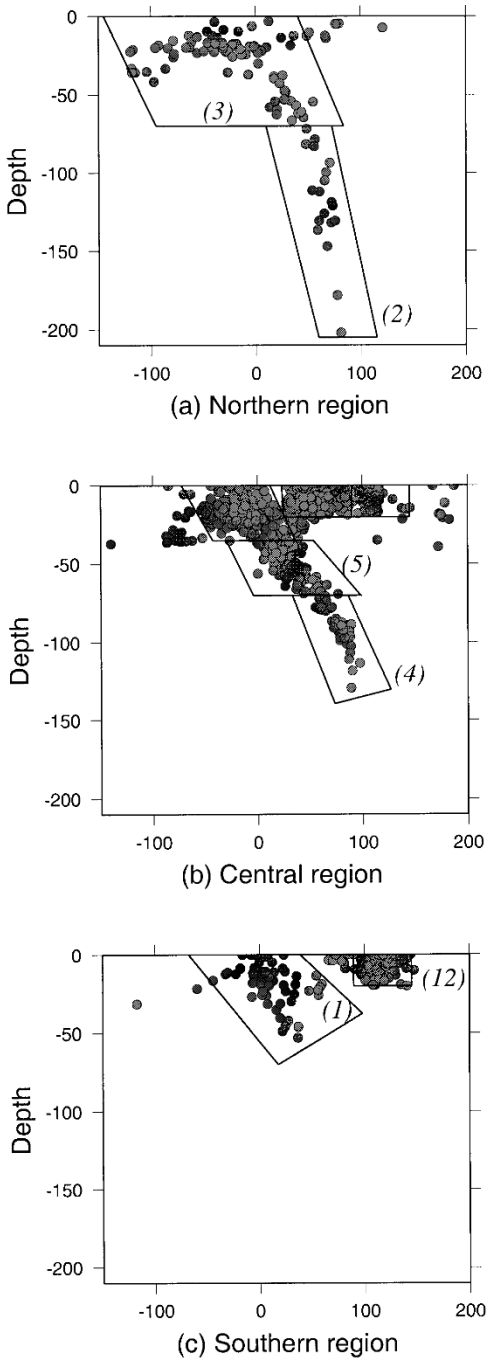

Figure 6. A cross-sectional view of earthquake hypocenters given in Figure 2. These depth distributions represent: (a) the northern seismicity, with epicenters north of line B; (b) central seismicity, which includes events between line A and B; and (c) southern Costa Rica seismicity, with events south of line A. Illustration of some selected seismic zones are shown.

Table 1. Velocity models used in this study

Model	Layer	Vp (km/sec)	Thickness (km)
MM	1	5.10	8.2
	2	6.20	12.9
	3	6.60	22.3
	4	7.85	16.6
	5	8.15	–
A1	1	5.10	2.0
	2	5.40	2.0
	3	6.00	4.2
	4	6.20	5.8
	5	6.30	4.0
	6	6.40	4.0
	7	6.60	4.0
	8	7.00	9.0
	9	7.80	15.0
	10	7.86	10.0
	11	7.90	20
	12	8.00	–
AP	1	5.90	25.0
	2	6.60	10.0
	3	7.90	–

in the seismicity profiles, between the central and southern segments, is shown by line A in Figure 4. For convenience, we made this line parallel to line B and approximately to coincide with the northwester flank of the Cocos Ridge. Therefore, this anomaly denotes the contrast of subducting oceanic lithosphere of different geological ages, as indicated above.

Relocated events have a relatively homogenous distribution in the upper 20-km within the continental crust. Below this depth, relocated earthquakes are mainly concentrated along the main thrust zone and within the subducted Cocos plate. The intermediate-depth earthquakes on the central and northern seismic zone are located in a very narrow band (see Figure 6). Here the deepest events are concentrated beneath the northern segment. For the central segment, earthquakes are located near the QSC feature with maximum depths reaching 120 km, approximately.

This study shows that relocated earthquakes in southeastern Costa Rica have shallow hypocenters. This seismicity is mainly associated with the shallow underthrusting of the Cocos plate and Cocos Ridge beneath the Caribbean plate (i.e. Panama Block).

Table 2. Results of the stress inversion for the 12 selected regions. N and R, are, respectively, the number of events in each group and the relative magnitude of the principal stresses corresponding to the obtained stress solution. P is the maximum stress, T the minimum and B the null axis. AZ is the azimuth and PL the plunge, in degrees. Latitude north and longitude west delimits the area. The stress regime categories include normal faulting (NF), predominantly normal with strike-slip component (NS), strike-slip faulting (includes minor normal or thrust component) (SS), thrust faulting (TF), predominantly thrust with strike-slip component (TS). Definition is according to Zoback (1992)

Region	Depth (km)	Area	N	R	P		T		B		Regime
					AZ	PL	AZ	PL	AZ	PL	
(1)	0–60	7.5–9.1 82.6–83.8	40	0.11	35	0	125	70	305	20	TF
(2)	>70	9.7–11.3 84.5–85.9	16	0.86	201	25	322	48	94	31	TS
(3)	0–70	9.7–11.3 84.5–85.9	80	0.33	221	27	349	50	116	27	TF
(4)	>70	9.1–10.3 83.6–84.7	46	0.83	183	39	343	49	84	10	TF
(5)	35–70	9.1–10.3 83.6–84.7	90	0.22	247	50	10	24	115	29	NS
(6)	0–35	9.1–9.7 84.4–85.2	200	0.33	225	10	346	72	132	15	TF
(7)	0–35	8.5–9.7 83.7–84.4	154	0.47	218	34	105	30	344	42	TS
(8)	0–20	9.7–10.0 84.2–84.5	174	0.78	16	23	276	20	150	58	SS
(9)	0–20	10.0–10.4 83.7–84.5	48	0.33	168	15	258	0	348	75	SS
(10)	0–20	9.6–9.9 83.8–84.1	88	0.50	218	30	101	38	334	38	SS
(11)	0–20	9.4–10.0 83.4–83.8	17	0.83	34	50	128	3	220	40	NS
(12)	0–25	9.2–10.3 82.5–83.6	154	0.53	6	26	113	30	243	49	SS

Intraplate seismicity is essentially observed along the central part and southeast of the back-arc of Costa Rica, and generally is manifested by shallow earthquakes, with depths less than 20 km (see Figures 4 and 6). We also, observe a cluster of events offshore northeastern Costa Rica and fewer events further beneath the Caribbean Sea. These latest events may be associated with deformation along the Hess scarp.

Earthquake stress field

In order to study the stress field by means of earthquake data, we divided the reviewed region into different zones. With the aid of earthquake locations given in previous section and tectonics of the region we choose 12 zones for investigation (see Escalante, 1990; Mann, 1995, for a geological and tectonic description of Costa Rica). The proposed zones of study are shown on Figure 4 and 6. We have tried to do one's best choosing zones: (a) along the frontal arc and within the subducted slab, (b) in the volcanic arc and (c) in the back arc of Costa Rica. The selected area and the number of P-wave polarities in the chosen zone will affect the stress results, and therefore other researcher could obtain different result for the same region. We believe that selected zones of study will give a good idea of stress tensor and fault plane orientation for the region. Table 2 shows results of the best-estimated values of orientation of the principal stress tensors. Figure 7 shows the orientation of principal stresses σ_1 and σ_3 of Table 2. White dots indicate the minimum stress axis (σ_3) and a black dot indicate the maximum stress axis (σ_1). Figure 8

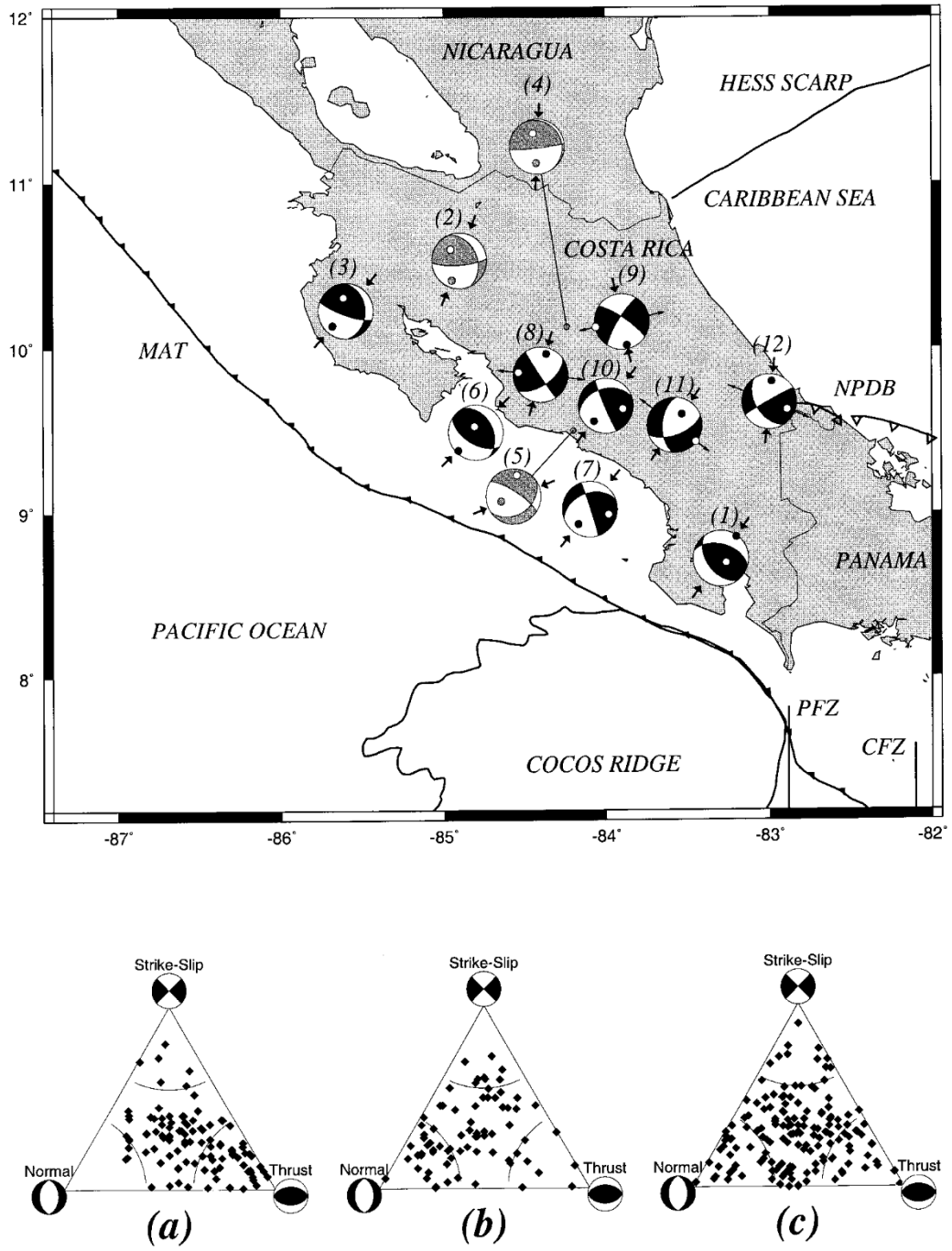

Figure 7. Equal-area projections showing orientation of principal stresses σ_1 and σ_3. The text above each ball indicates the zone according to Table 2. White dots indicate the minimum stress axis (σ_3) and a black dot indicate the maximum stress axis (σ_1). The direction of σ_1 and σ_3 are indicated by thick and thin arrows, respectively. The stress tensor was obtained from a set of polarities of P wave first motion for different zones as explained in the text. Different shadings inside the darkness quadrants indicate groups with different depth, as explained in text figure 5. Also are shown triangle diagrams for displaying earthquakes focal mechanism (see Frolich and Apperson, 1992). Solutions having less uncertainty in the determination of P and T axes are shown on the triangles. The interplate events are represented in triangle (a) (zones 1, 2, 3, 4 and 6), they are characterized by thrust faulting and triangle (b), which represent events in zones 5 and 7. Normal, strike-slip and thrust fault mechanisms are presented in this area. The triangle (c) represent intraplate events (zones 8–12) and all types of fault mechanisms are represented in this area.

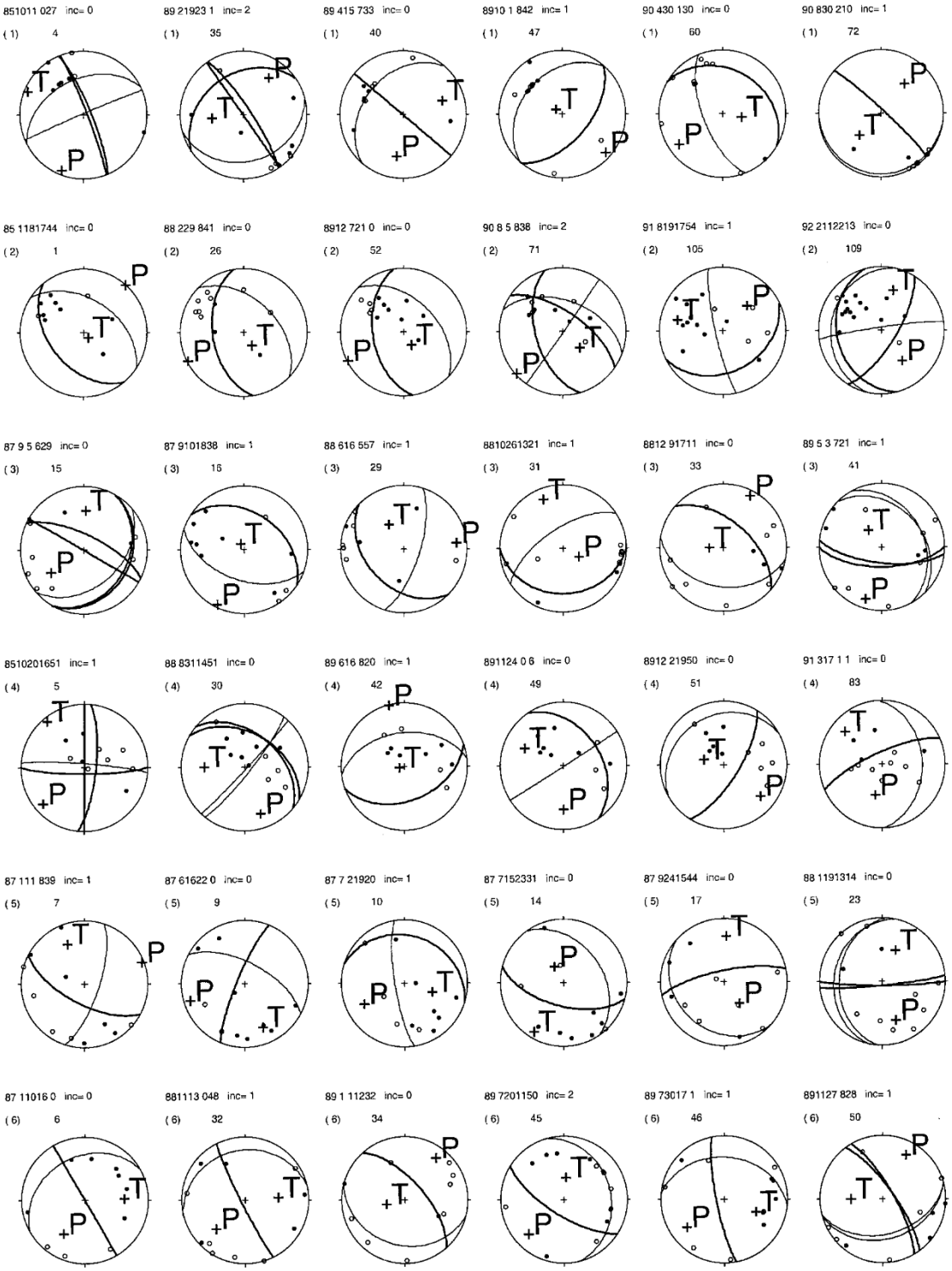

Figure 8. Equal-area projection showing the orientation of fault planes for events occurring in zones shown in Figure 4. Either a solid (compression) circle or open circle (dilatation) indicates P-wave polarity. The label above each mechanism gives the origin time of the earthquake, the number of inconsistent polarities (inc) and the identification zone number. The identification number refers to Table 3.

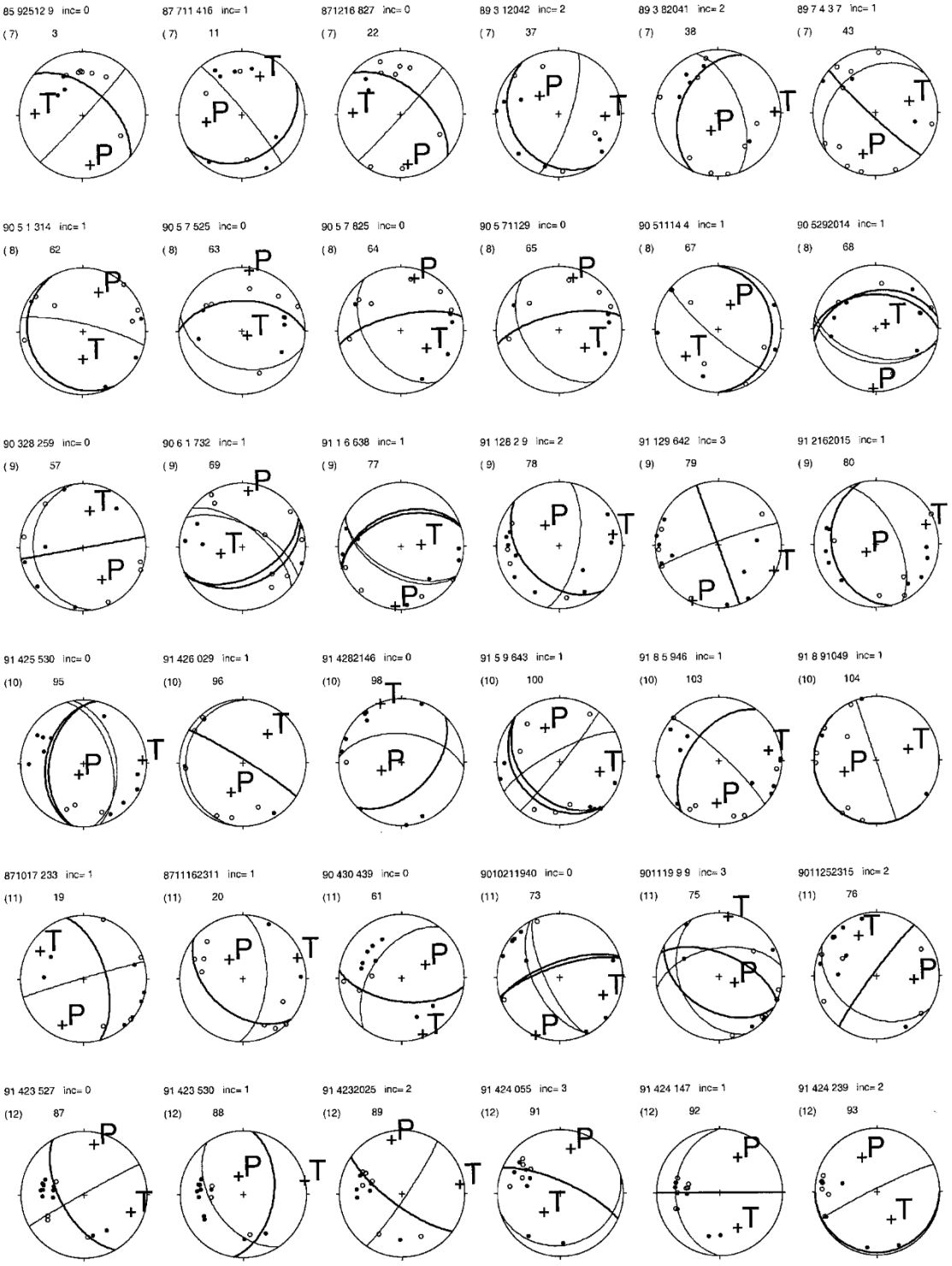

Figure 8. Continued

Table 3. Pressure and Tension axes of 118 earthquakes in the Costa Rica region. N refers to number of polarities used for the focal mechanism solution and Mc is the local earthquake magnitude

Year	Mo	Day	Hr	Min	Latitude	Longitude	Focal	P-axes		T-axes		Mc	N	No.
					Deg. N°	Deg. W°	Depth	Azimuth	Plunge	Azimuth	Plunge			
1985	1	18	17	44	10.415	–85.020	81.6	42	1	136	82	4.1	10	1
1985	9	3	0	29	10.122	–85.780	21.9	215	49	29	41	4.3	10	2
1985	9	25	12	9	9.004	–84.109	0.5	171	22	273	26	4.6	10	3
1985	10	11	0	27	8.591	–83.592	8.6	202	8	293	6	3.9	10	4
1985	10	20	16	51	10.135	–84.152	93.2	229	15	321	7	3.1	10	5
1987	1	10	16	0	9.252	–84.868	26.5	213	37	87	37	3.8	10	6
1987	1	11	8	39	9.453	–84.253	37.5	236	32	351	34	3.5	11	7
1987	6	2	3	11	9.041	–83.874	25.8	243	51	27	34	4.6	10	8
1987	6	16	22	0	9.329	–84.212	47.2	63	20	327	15	3.7	10	9
1987	7	2	19	20	9.403	–84.000	59	232	29	80	59	3.7	11	10
1987	7	11	4	16	9.086	–84.091	25.5	259	43	26	33	3.2	10	11
1987	7	15	11	36	9.492	–84.163	46.2	262	25	148	42	4.4	13	12
1987	7	15	14	31	9.508	–84.148	43.8	248	12	116	73	4.3	11	13
1987	7	15	23	31	9.528	–84.153	41.5	314	59	210	8	4.1	11	14
1987	9	5	6	29	9.745	–84.807	19.6	236	38	3	38	2.8	10	15
1987	9	10	18	38	10.107	–84.824	54	206	6	334	81	3.8	11	16
1987	9	24	15	44	9.813	–84.480	41.8	137	66	358	19	3.3	10	17
1987	9	27	21	19	10.458	–86.048	19.1	350	40	229	31	4.9	11	18
1987	10	17	2	33	9.61	–83.571	10.2	205	22	304	19	3.6	11	19
1987	11	16	23	11	9.423	–83.530	18.9	326	60	69	8	3.2	10	20
1987	11	19	16	2	9.706	–83.559	10.2	23	37	230	50	4.3	12	21
1987	12	16	8	27	8.961	–84.110	20.6	171	22	273	26	3.2	10	22
1988	1	19	13	14	9.674	–84.132	43.3	149	33	24	42	3.6	11	23
1988	1	21	18	51	10.594	–85.091	136.7	137	45	317	45	4.5	10	24
1988	1	31	23	31	9.776	–83.606	1.9	71	42	289	42	4.5	12	25
1988	2	29	8	41	10.485	–85.102	71.9	243	2	148	70	3.7	11	26
1988	3	2	7	13	9.479	–84.900	23.8	16	35	171	52	4.7	12	27
1988	5	19	9	29	10.424	–84.667	118.6	114	41	299	49	4.8	11	28
1988	6	16	5	57	10.053	–84.989	39.7	83	17	330	53	3.4	10	29
1988	8	31	14	51	10.211	–84.169	100.4	161	23	270	37	4.0	12	30
1988	10	26	13	21	10.098	–85.713	35.7	117	67	338	18	3.9	11	31
1988	11	13	0	48	9.469	–84.691	16	225	37	85	46	2.6	11	32
1988	12	9	17	11	9.683	–84.917	27.9	28	8	270	73	3.3	11	33
1989	1	1	12	32	9.618	–84.929	20.6	37	19	257	66	3.1	10	34
1989	2	19	23	1	8.899	–83.315	42.2	35	30	264	48	3.4	11	35
1989	2	26	12	21	9.652	–84.193	18.5	201	42	87	25	4.4	15	36
1989	3	1	20	42	9.659	–84.213	15.6	314	56	93	27	2.7	11	37
1989	3	8	20	41	9.222	–83.978	19.6	201	66	89	10	3.2	13	38
1989	4	2	10	35	10.709	–85.923	58	222	55	28	35	5.2	12	39
1989	4	15	7	33	8.986	–82.978	20.8	189	35	71	35	3.2	10	40
1989	5	3	7	21	9.652	–84.877	24.7	197	17	322	62	3.5	11	41
1989	6	16	8	20	10.216	–84.190	89.5	346	0	253	84	3.1	10	42
1989	7	4	3	7	9.233	–84.311	15.1	197	33	72	42	3.5	13	43
1989	7	20	5	2	10.714	–85.227	130.7	192	33	78	33	4.3	13	44
1989	7	20	11	50	9.322	–84.806	30.4	226	23	6	61	3.2	14	45
1989	7	30	17	1	9.556	–84.870	18.5	234	28	111	45	3.3	12	46
1989	10	1	8	42	8.293	–82.841	18.7	131	10	310	80	4.7	12	47

Table 3. Continued

Year	Mo	Day	Hr	Min	Latitude Deg. N°	Longitude Deg. W°	Focal Depth	P-axes Azimuth	P-axes Plunge	T-axes Azimuth	T-axes Plunge	Mc	N	No.
1989	11	3	0	59	8.48	–2.846	48.8	135	45	315	45	4.5	11	48
1989	11	24	0	6	10.209	–84.323	87.5	180	32	294	34	3.3	10	49
1989	11	27	8	28	9.638	–84.877	12.1	29	22	271	48	2.9	10	50
1989	12	2	19	50	10.216	–84.137	88.7	130	24	286	64	3.4	11	51
1989	12	7	21	0	10.593	–84.997	125.9	243	2	148	70	4.0	12	52
1989	12	19	17	26	8.375	–82.996	25.7	104	48	302	40	4.5	12	53
1990	2	16	7	49	8.536	–83.171	21.9	13	26	207	64	4.7	13	54
1990	3	25	21	35	9.407	–84.807	25.8	210	5	355	84	4.7	15	55
1990	3	27	14	52	9.433	–84.782	21.5	256	5	32	83	4.4	13	56
1990	3	28	2	59	10.124	–84.030	6.7	149	41	11	41	2.7	11	57
1990	4	3	11	52	9.943	–85.946	23.2	35	25	203	64	4.4	15	58
1990	4	28	1	23	8.728	–83.585	13.8	33	16	185	72	5.5	13	59
1990	4	30	1	30	8.776	–83.523	10.9	235	19	99	65	3.3	10	60
1990	4	30	4	39	9.565	–83.531	0.1	61	54	159	6	2.9	11	61
1990	5	1	3	14	9.816	–84.302	6.5	22	34	180	54	2.2	10	62
1990	5	7	5	25	9.838	–84.316	0.5	7	5	128	81	2.5	12	63
1990	5	7	8	25	9.832	–84.321	3.6	15	16	124	49	2.4	12	64
1990	5	7	11	29	9.837	–84.320	3	15	16	124	49	2.4	10	65
1990	5	10	21	15	9.401	–84.841	20.1	332	71	119	16	4.5	11	66
1990	5	11	14	4	9.744	–84.306	7.5	28	54	231	34	2.5	10	67
1990	5	29	20	14	9.835	–84.301	1.5	182	7	65	76	2.5	11	68
1990	6	1	7	32	10.055	–84.059	10.9	7	12	254	61	3.1	13	69
1990	6	9	0	34	9.865	–84.311	12.4	9	16	247	61	4.4	16	70
1990	8	5	8	38	10.526	–84.785	121	228	3	133	60	3.4	11	71
1990	8	30	2	10	8.58	–83.009	40.4	39	40	226	50	3.8	10	72
1990	10	21	19	40	9.611	–83.588	6.8	203	2	112	27	2.9	11	73
1990	11	9	21	11	8.871	–84.260	16.7	243	19	145	23	4.3	13	74
1990	11	19	9	9	9.628	–83.666	10.8	109	69	9	4	2.6	12	75
1990	11	25	23	15	9.621	–83.653	6.1	95	39	336	31	2.5	14	76
1991	1	6	6	38	10.039	–84.193	6.1	186	6	84	64	2.5	11	77
1991	1	28	2	9	9.974	–83.827	3.2	325	57	78	14	3.1	14	78
1991	1	29	6	42	9.978	–83.831	6.6	205	3	115	3	3.1	14	79
1991	2	16	20	15	10.043	–84.174	2.8	232	74	69	15	3.0	14	80
1991	3	16	6	2	9.682	–85.711	19.8	203	44	322	27	5.1	15	81
1991	3	16	6	32	9.834	–85.706	22.1	198	30	10	59	4.3	14	82
1991	3	17	1	1	9.954	–84.246	72.2	192	49	312	23	3.2	12	83
1991	3	22	4	58	9.527	–84.680	27.8	33	22	184	65	4.4	14	84
1991	4	23	18	56	9.833	–83.169	4.6	24	45	204	45	4.4	13	85
1991	4	23	8	32	9.73	–83.209	0.1	135	45	315	45	4.3	15	86
1991	4	23	5	27	9.823	–83.364	0.1	12	19	110	22	3.7	16	87
1991	4	23	5	30	9.841	–83.316	0.9	346	66	77	0	3.5	15	88
1991	4	23	20	25	9.485	–83.031	1.1	349	15	81	7	3.6	13	89
1991	4	24	19	12	9.585	–83.548	3.5	38	48	225	42	4.9	11	90
1991	4	24	0	55	9.262	–83.123	2.8	14	29	221	58	3.0	12	91
1991	4	24	1	47	9.787	–83.106	1	27	37	153	37	3.4	14	92
1991	4	24	2	39	9.846	–83.153	5.2	336	41	152	50	3.2	11	93
1991	4	25	2	47	9.792	–83.212	3.2	122	82	254	5	4.3	15	94
1991	4	25	5	30	9.705	–83.995	17.1	203	75	87	7	3.5	13	95

Table 3. Continued

Year	Mo	Day	Hr	Min	Latitude	Longitude	Focal	P-axes		T-axes		Mc	N	No.
					Deg. N°	Deg. W°	Depth	Azimuth	Plunge	Azimuth	Plunge			
1991	4	26	0	29	9.812	–83.928	5.7	201	49	41	39	2.8	10	96
1991	4	27	5	42	10.139	–83.302	21.5	19	0	289	54	4.6	15	97
1991	4	28	21	46	9.686	–83.874	7.4	248	62	340	1	2.8	10	98
1991	4	29	22	48	9.594	–82.915	11.8	71	54	244	36	4.3	14	99
1991	5	9	6	43	9.731	–83.915	13.9	337	41	104	35	3.2	12	100
1991	6	22	2	23	9.833	–83.106	0.1	17	45	197	45	4.3	13	101
1991	7	9	8	59	9.648	–82.998	0.1	43	20	147	35	4.3	12	102
1991	8	5	9	46	9.736	–84.038	11	183	34	78	21	3.0	16	103
1991	8	9	10	49	9.74	–84.047	7.1	251	45	71	45	2.6	11	104
1991	8	19	17	54	10.125	–84.526	77.7	44	44	284	28	3.9	15	105
1991	9	13	1	34	9.948	–85.696	17.1	15	20	148	61	4.8	17	106
1991	9	23	15	16	9.393	–84.626	17.1	114	25	296	65	4.4	16	107
1991	10	9	6	30	10.148	–84.282	87.3	230	3	332	75	4.3	14	108
1992	2	11	22	13	10.508	–84.950	111.9	144	42	17	34	4.0	16	109
1993	2	16	18	33	10.751	–85.021	178.2	135	45	315	45	4.5	15	110
1993	7	10	20	40	9.762	–83.667	13.9	5	63	118	11	4.4	16	111
1993	9	4	22	46	10.857	–85.109	202	167	45	347	45	4.8	14	112
1994	10	31	22	59	8.795	–83.450	19.7	288	45	108	45	4.6	11	113
1994	12	28	21	22	9.547	–84.351	20.9	220	65	69	22	4.5	14	114
1995	2	28	5	3	11.25	–86.039	111.1	45	29	182	52	5.3	12	115
1995	5	23	8	31	8.978	–84.047	15.4	49	28	254	60	4.3	11	116
1995	7	23	1	23	10.824	–85.138	199.1	46	35	226	55	5.1	14	117
1996	2	22	8	38	8.546	–83.217	12.2	188	45	8	45	4.4	13	118

shows examples of focal mechanism solution determined with stress solutions. Table 3 summarizes the focal mechanism results, listing date, origin time, hypocenter location, P-axes, T-axes, number of polarities and local magnitude.

Frontal Arc and Subduction segments

Zone 1: The seismicity in this area is mainly associated with the shallow underthrusting of Cocos Ridge beneath the Caribbean plate. The axis of MAT meets the PFZ in southwestern of this zone, offshore the Burica peninsula. This fracture zone separate the Cocos plate from the Nazca plate, forming together with the Caribbean plate an unstable triple junction (Molnar and Sykes, 1969). The PFZ is a right lateral north trending transform fault, that divides into at least two faults north of 6°N, i.e into the Coiba Fracture Zone (CFZ) and Balboa Fracture zone (BFZ) (Adamek et al., 1988). One of the latest destructive earthquakes in the area occurred on April 3, 1983 (Ms = 7.3). The source mechanism indicated that the event was a thrust event along the MAT (Adamek et al., 1987). For the stress inversion in this area, we used data in the depth range 0 to 60 km. The result indicated a maximum stress σ_1 oriented NE-SW and a dip angle almost horizontal (Figure 9). The direction of the maximum stress is close to the direction of the motion of the Cocos and Caribbean plates (i.e. Panama Block). The mechanisms of the studied earthquakes are fundamentally thrust faults with a small component of strike-slip motion (see Figure 8 and 10).

Zone 2: This zone is located in northwestern Costa Rica and includes events with depth $\geq$ 70 km. Isacks and Molnar (1971) recognized the subduction zone of Central America as downdip extension. In other words, the deepest events in this area have tension axis approximately parallel to the dip of the slab (see Lay and Wallace, 1995, page 457). Our result indicated that this zone has the maximum stress with orientation NE-SW and the minimum stress sub-vertical. The subducted slab shows predominantly thrust faulting with extensional stresses oriented in the down dip direction.

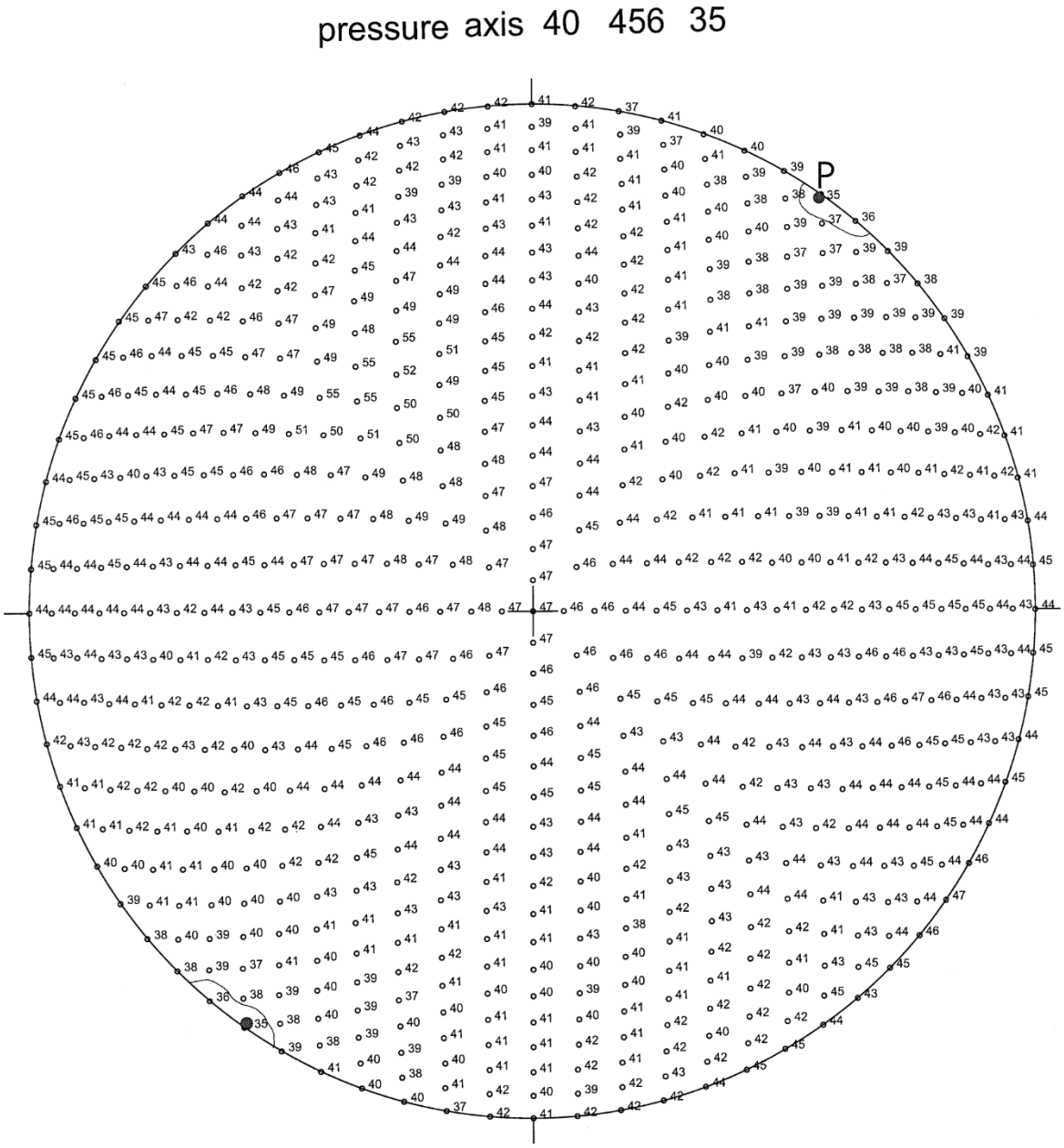

Figure 9. Obtained orientation of the maximum principal stress in zone 1. The numbers indicated the number of inverted events (40), polarity readings (456) and the minimum number of inconsistent stations (35) for the best model. The contour line indicates where the total number of inconsistent stations is 36, approximately.

Zone 3: This zone is located also in northwestern Costa Rica and the selected area is wider to include enough P-wave polarity data. A large shallow thrust earthquake (Ms = 7.0) occurred on August 23, 1978 in this zone (9.76°N, 85.57°W). It had source geometry consistent with the subduction of the Cocos plate under the Caribbean plate along a shallow thrust fault dipping 22° in a N28°E direction (Güendel and McNally, 1982). For events with depths between 0–70 km, a compressional characteristic is observed, with σ_1 oriented along an azimuth of N221° and dip-

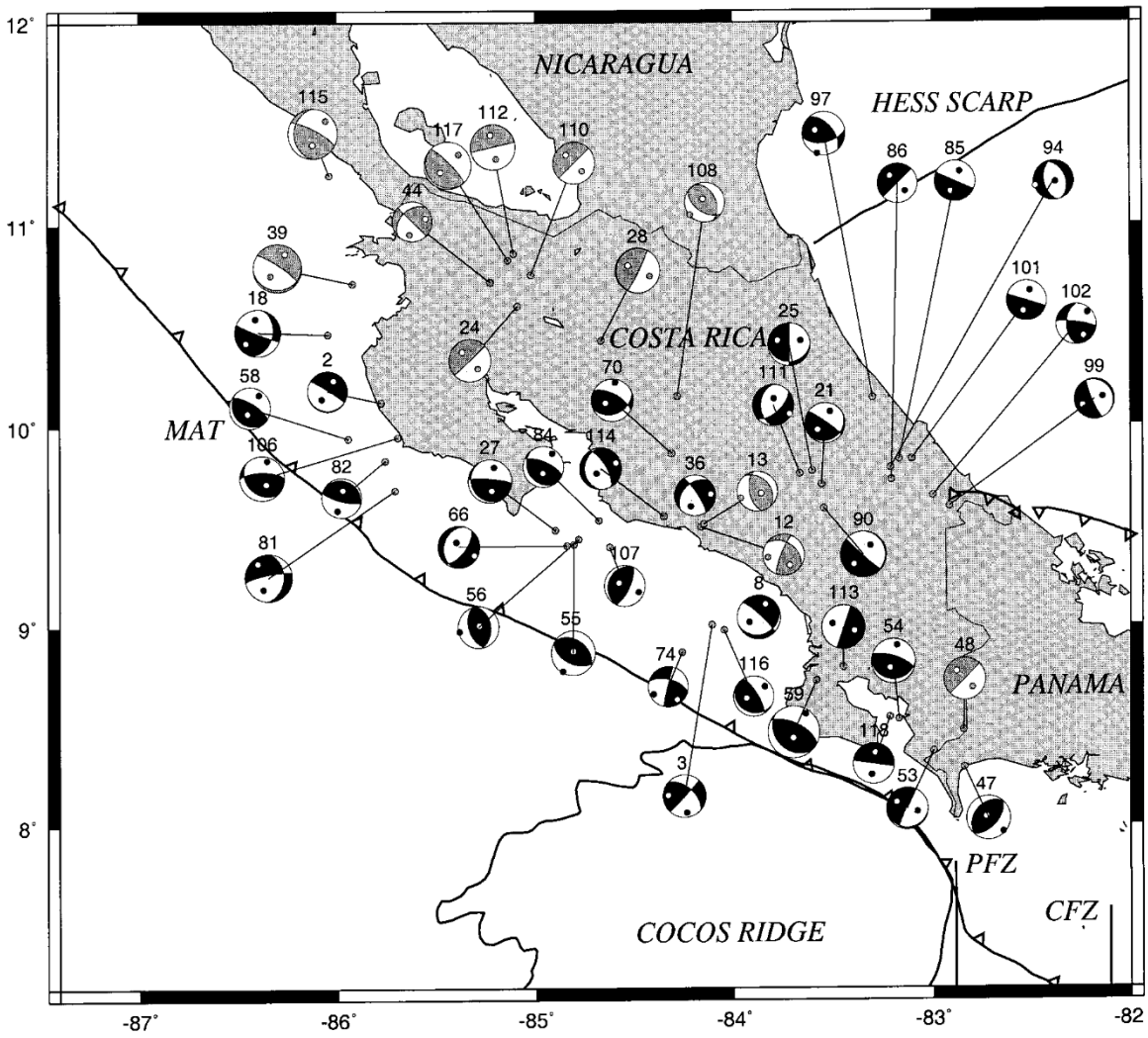

Figure 10. Lower hemisphere focal mechanism solution of some events with magnitude ≥ 4.3 shown in Figure 2. Solid quadrants are compressional P-wave first motions, with a white dot indicating the tension axis; white quadrants are dilatational P-wave first motions, with a black dot indicating the compression axis. Different shadings inside the darkness quadrants of plotted focal mechanism correspond to 0–35 km depth for black and 35–250 for grey shaded focal mechanism.

ping 27°. In general, the northern subduction zone shows a compressive or thrust type stress regime.

Zone 4: The chosen zone is located within the Cocos subducted slab in central Costa Rica. The deepest events of this region between lines A and B are concentrated beneath the central volcanic chain (see Figure 4). A segmentation or tear in the subducted slab is expected in this area (Güendel and Protti, 1995; Colombo et al., 1997). Our hypocenter location show that the dipping slab in central Costa Rica is different compared with the northwestern part (see Figure 6). The stress analysis comprises events with focal depths between 70 and 125 km. Our results show a thrust type stress regime within the subducted Cocos plate for the central region of Costa Rica. The parameters of this stress tensor correspond to thrust and normal earthquakes with a strike-slip component. Strike-slip component and mechanism in this area can be a direct result of the tear or segmentation within the subducted plate.

Zone 5: South of the central volcanic chain, earthquake depths within the subducting slab decrease considerably. In our case, the projection along the northern flank of the Cocos Ridge (line A) serves as

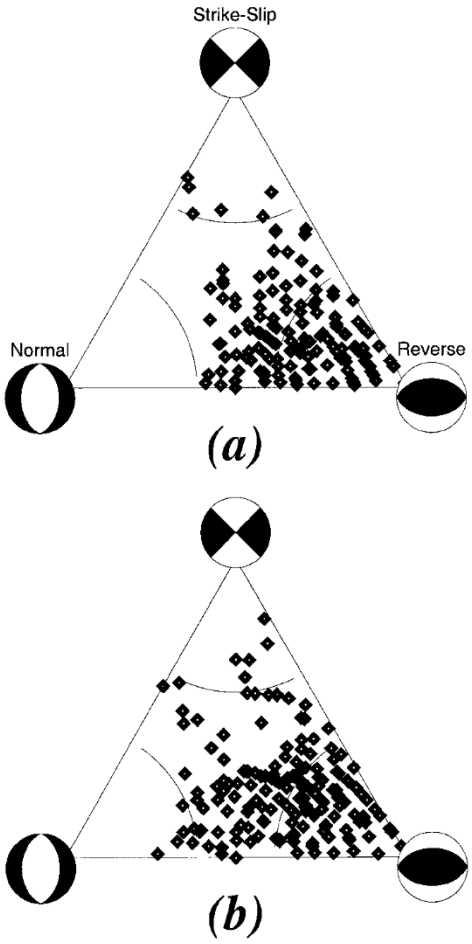

Figure 11. Triangle diagrams displaying earthquakes focal mechanism for zone 6 (Cobano). (a) Mechanism calculated using the A1 model and the JHD location. (b) Mechanism calculated using A1 model and initial earthquake locations.

the limit of the deepest events of the central region of Costa Rica. The zone comprises events whose depths are between 35 and 70 km. Von Huene et al. (1995), and Dominguez et al. (1998), indicated that this area is characterized by the subduction of the Quepos plateau and other seamount domains, which cause normal and strike-slip faulting. Our mechanism solutions also give evidence of thrust and normal faults with strike-slip components (see Figure 7).

Zone 6: Earthquakes concentrated in the central part of Costa Rica, offshore of the Pacific coast (depth $\leq$ 35 km) are mainly associated with the subduction zone. A large thrust earthquake occurred, on March 25, 1990 (Ms = 7.0), within this area. Its aftershock zone did not extend beyond 35 km in depth (Protti and McNally, 1990), and their epicenters were mainly located east of line B (Figure 4). The amount of data collected by the network made it possible to choose a narrow region for stress investigation. Stress inversion shows that σ_1 is oriented along an azimuth of N225° and plunging 10°. Earthquakes in this region are characterized by reverse faulting (see Figure 10 and 11).

Zone 7: This zone is located in central Costa Rica off Pacific coast and northwest of the Cocos Ridge. Result provided the maximum stress-axis oriented NE-SW. Patterns of reverse and normal faulting with a strike-slip component characterize the solutions obtained for this area (see Figure 7). The normal and strike-slip faulting, found for this zone, are related to the subduction and deformation of seamount chains parallel with the northwestern flank of the Cocos Ridge (Von Huene et al., 1995).

In general, the frontal convergence zone in Costa Rica (convergence of the Cocos and Caribbean plates, area along the Pacific coast of Costa Rica) displays compressive seismic deformations in NE-SW direction, i.e. the area between the trench axis and the coast is mainly exposed to compression with predominance of thrust faulting. However, we found some indication of normal and strike-slip faulting, for the area indicated by zone 7. The different types of faults associated with this region are related to the subduction and deformation of a seamount chain that parallels the northwestern flank of the Cocos Ridge (Von Huene et al., 1995).

Volcanic and back-arc zones

The intraplate Caribbean seismicity in the Costa Rican region is concentrated along the central (volcanic arc) and southeastern parts (back-arc) of Costa Rica. Since the majority of seismic stations are concentrated in central Costa Rica, the seismicity in this area is well monitored. Therefore, we were able to choose different, narrow zones in this region for stress inversion.

Zone 8: This zone (Puriscal zone) is located around 40-km trenchward of the volcanic front and earthquakes studied in this area are mostly associated with the 1990 seismic sequence, which started on March 26, 1990. Two major events on June 30, 1990 (Ms = 5.1) and on December 22, 1990 (Ms = 5.7) occurred in this zone. These events had strike-slip mechanisms, with a strike of N60°E, approximately (Fan et al., 1993). Stress inversion results for this zone

show that maximum and minimum stresses are nearly horizontal, oriented in the N-S and E-W direction. There are earthquakes that display left-lateral (LLSS) and right-lateral (RLSS) strike-slip components. The LLSS fault planes are oriented in a NE-SW direction, and the RLSS in a NW-SE direction. In general we can say that these events predominantly show shallow strike-slip fault plane solutions, with smaller thrust and normal components.

Zone 9: This zone includes an active volcanic range in central Costa Rica. Previous stress analysis for the region, using the spatial distribution of dikes, monogenetic cones, and faulting suggests a gradually more compressive environment along the strike of volcanic arc from southern Nicaragua to central Costa Rica (Nakamura, 1977). The last author found that the direction of the maximum horizontal stress in central Costa Rica is N-S oriented at the volcanic front and in the back-arc. Results of the inversion show a maximum stress component approximately in the N-S direction with horizontal dip angle, while σ_2 is almost vertical. In general, all types of faults characterize this region. The thrust faults and strike-slip faults of this area are associated with the formation of the volcanic chain.

Zone 10: This zone is located between the frontal and volcanic arc of central Costa Rica. Focal mechanism for the February 26, 1990 (Ms = 4.8) and August 9, 1991 (Ms = 4.7) events in this zone suggest a strike-slip fault with NE-SW compression and E-W tension (Fan et al, 1993). The stress inversion indicates that σ_1 has an azimuth of N218° and sub-horizontal dipping plane and the minimum principal stress is oriented in the E-W direction. Fault plane solutions for events in this zone show diverse types of faulting with normal, thrust, strike-slip and oblique faulting.

Zone 11: Zone located in central Costa Rica with east border terminated by a projection of the Cocos Ridge (line A, Figure 4). In this zone an intraplate earthquake occurred on July 3, 1983 (Ms = 6.2). The focal mechanism reveals an oblique strike-slip fault. The stress inversion for this zone shows a stress regime predominantly normal with a strike-slip component and σ_1 nearly vertical and the direction of the minimum stress being NW-SE. Focal mechanisms of studied earthquakes provide fundamentally normal events. There are also focal mechanisms that indicate strike-slip or oblique strike-slip faults (see Figure 12a). This

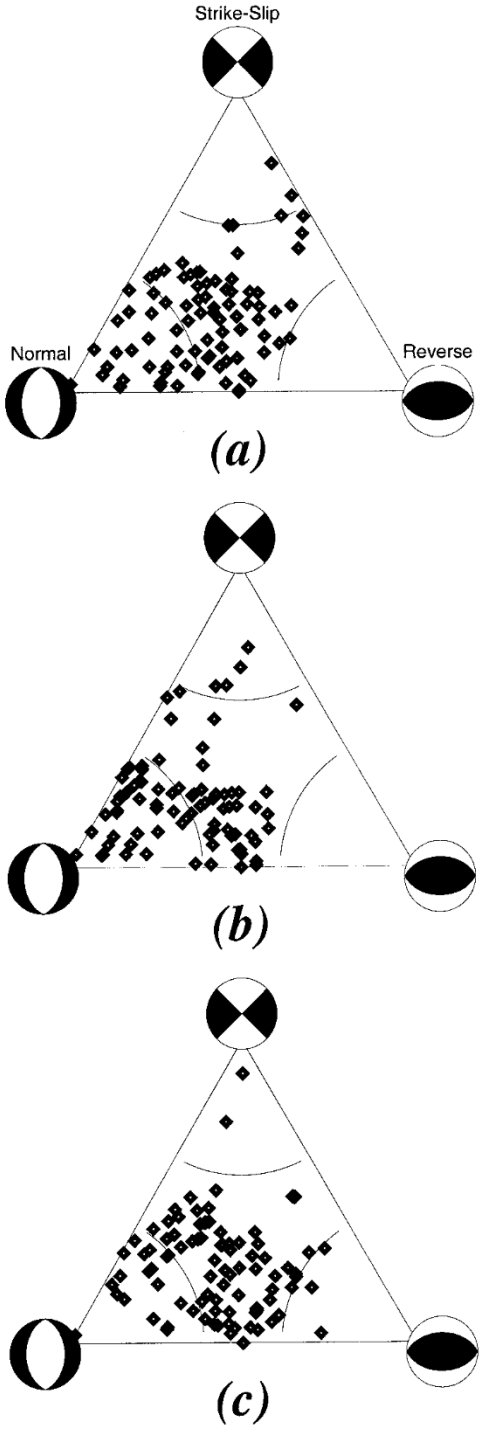

Figure 12. Triangle diagrams displaying earthquakes focal mechanism for zone 11. (a) Mechanism calculated using the A1 model and the JHD location. (b) Mechanism calculated using AP model and initial earthquake locations. (c) Mechanism calculated using mm model and initial earthquake locations.

finding is in accordance with the results of Fan et al. (1993), presenting a predominance of strike-slip or oblique faulting northwest of the Valle de la Estrella.

In general the intraplate Caribbean seismicity in the volcanic arc of central Costa Rica shows predominant shallow left-lateral strike-slip focal mechanism solutions (although normal and thrust faults are also present). This is in agreement with the expected left-lateral motion for central Costa Rica along the proposed shear zone (Güendel et al., 1992; Fan et al., 1993; Schwartz, 1995). It is also, possible to associate the RLSS fault plane of the Puriscal area with the dextral longitudinal fault zone (Ballena Celmira Fault Zone, BCFZ) that runs parallel to the trench from Panama to central Costa Rica (Kolarsky et al., 1995). Our analysis suggests that events along the arc and events associated with the North Panama Deformed Belt (NPDB) have the maximum stress axes in NEE-SWS direction with horizontal or sub-horizontal dipping angles. The stress regime corresponds to a compressive zone.

Zone 12: This zone includes earthquakes located in the backarc of Costa Rica i.e. mainly aftershocks of the Valle de la Estrella, April 22, 1991 mainshock (Mw = 7.7). This earthquake interpreted as a backarc shallow thrust event, occurred on a shallow southwest dipping plane with a small oblique component and related to the NPDB. Most likely, the location of this event represents the termination of the NPDB (Goes et al., 1993). The termination of the NPDB occurs in a diffuse zone of strike slip faulting. This deformation zone in central Costa Rica is characterized by left-lateral strike-slip motion, striking in northeast-southwest direction. It connects the NPDB with the MAT (Guendel et al., 1992; Fan et al., 1993; Schwartz, 1995). Our result determines the maximum principal stress with a shallow dip angle of 26° and N-S oriented. Thrust, strike-slip and normal faults represent the focal mechanism solutions of this zone (see Figure 7, 8 and 13). This seismicity corresponds mainly to internal deformation along the collision zone and occurs along shallow left-lateral strike slip faults. Although focal mechanism solutions show that all types of faults are present, thrust and left-lateral strike slip faults are the dominant feature in the southeastern part of the back-arc region. Strike slip faults are striking in a NE-SW direction.

In general, the southeastern part of the back-arc region of Costa Rica shows a compressive pattern with the maximum stress nearly horizontal and parallel to

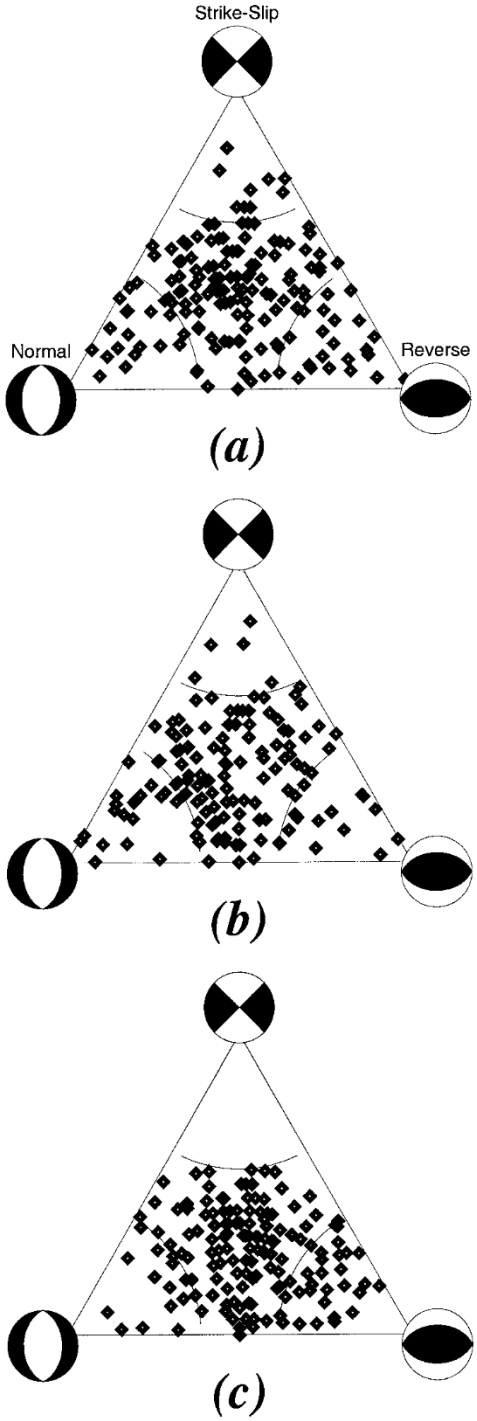

Figure 13. Triangle diagrams displaying earthquakes focal mechanism for backarc zone (12) of Costa Rica (Limon). (a) Mechanism calculated using the A1 model and the JHD location. (b) Mechanism calculated using AP model and initial earthquake locations. (c) Mechanism calculated using MM model and initial earthquake locations.

the convergence of the Cocos and Caribbean plates. We believe that the short scale tectonic complexity of Costa Rica and its vicinity is responsible for the diversity of focal mechanisms found in the study area.

In the final step of this work, we compared results when different velocity models and earthquake locations are used in the calculation of principal stresses and focal mechanism. Locations and models are used to calculate azimuths and take-off angles. In these tests we used the MM model and the initial location obtained with the MM model (Figure 3). We also tested the AP model shown in Table 1, proposed by Fan et al., (1993) for the NPDB region. Triangle diagrams for displaying earthquake focal mechanisms were used to exhibit the results. Figures 11, 12 and 13, display the results for zones 6, 11 and 12, respectively. Figure 11a and 11b were obtained using the A1 model with relocated events and the A1 model with initial location, respectively. In this figure we can observe from the triangular representation for the subduction zone 6 a clear indication of thrust faulting as the preferred mechanism. Figures 12a, 12b and 12c were obtained using the A1 model and relocated events, AP and MM models and the initial locations. These diagrams show that normal and strike-slip events are the dominant mechanisms inland, southwest of the termination of the NPDB. Figures 13a, 13b and 13c, display the results obtained for the area associated with the NPDB and obtained using relocated events and model A1, initial location and model AP and finally initial location and model MM, respectively. All these diagrams show that the area associated with the NPDB contains a mixture of all types of focal mechanism. However, when the MM model is used (Figure 13c), pure strike-slip mechanisms are less common for this area. We also carried out tests for the remaining areas indicated in Table 2, but results are not presented here. In general, there are agreements of the focal mechanisms represented in the triangle diagrams, although a single comparison may indicate a difference in the mechanisms. From this comparison, we conclude that the A1 velocity model and relocated events are adequate to constrain the fault plane geometry for the selected zones in Costa Rica.

Conclusions

The earthquake epicenters in Costa Rica and surrounding regions are mainly distributed along the subduction zone, along the Panama Fracture Zone, in a wide fan shaped shear zone that traverses central Costa Rica from west to east, along the NPDB and as a nest of earthquakes offshore of northeastern Costa Rica. The two latter groups of earthquakes are located along the Caribbean coast. The intraplate earthquakes occur mainly in the upper 20 km. Below 20 km depth, earthquake hypocenters are concentrated along the main thrust zone and within the subducted Cocos plate.

The seismicity associated with the under thrusting of the Cocos plate beneath the Caribbean plate shows mostly thrust focal mechanism components, with a compression component in the NE-SW direction. The intermediate-depth central subduction zone shows a thrust type stress regime with strike slip component, which could be caused by the tear formed between the northern and central subduction zone. A strike-slip stress regime and the tension axis striking in the E-W direction characterise the continental crust of the central part of Costa Rica. The back-arc region in southeastern Costa Rica shows a compression pattern. This zone is represented by thrust and strike slip faults.

Figure 14 summarizes our results. The compression directions of the maximum stress component, as indicated by thick black arrows, are almost perpendicular to the trench and parallel to the convergence direction of the two plates. The active volcanoes are shown by triangles and a thick line indicates the volcanic chain for northern and central Costa Rica. σ_2 is vertical in this volcanic area and the maximum stress component is horizontal with a north-south direction (Nakamura and Uyeda, 1980). The strike-slip stress pattern observed in this area is characteristic of the entire Central American volcanic chain (White and Harlow, 1993). The dotted line indicates the projection at depth where the QSC is to be found, separating the northern and central subduction zones. Faults interpreted from earthquake data are shown as continuous lines. The shear zone, although more complex than represented here, is indicated by a solid line. This line shows the northern boundary of this shear zone, and is represented by the inland projection of the ENFZ. The strike-slip pattern found along the Pacific coast (zone 5 and 7) and related to this shear zone, appears to be associated with subduction of the seamount domain beneath the Caribbean plate (see also, Dominguez, et al., 1998).

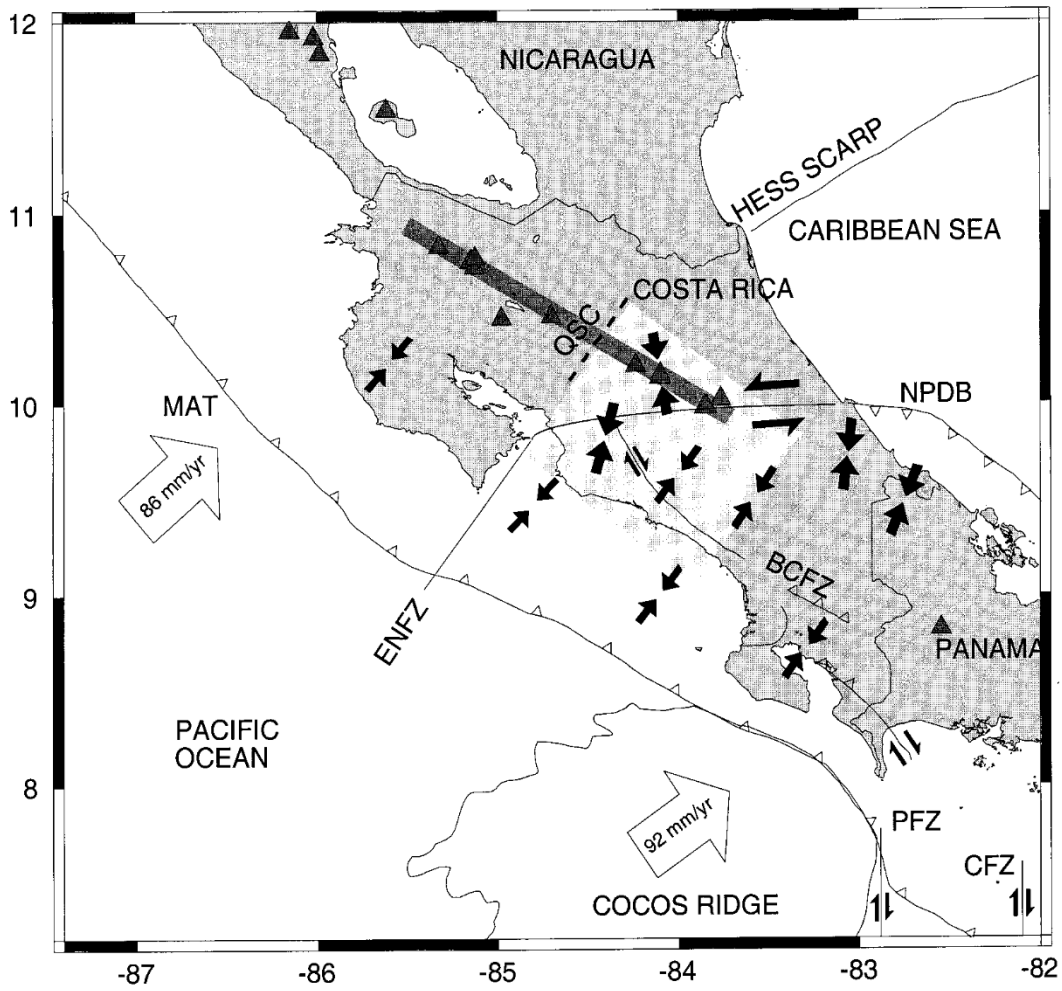

Figure 14. Summary of the results. Open arrows show the direction of convergence of the Cocos with respect to the Caribbean plate; the relative velocities for southern and northern Costa Rica are also indicated. Thick black arrows indicate the compression direction of the maximum stress component. The active volcanoes are marked by triangles and the thick line shows the volcanic chain in northern and central Costa Rica. The dotted line indicates the place where the northern and central subducted zone is believed to form a tear zone. The gray square in central Costa Rica represents the intraplate seismicity in this zone. Faults confirmed by earthquake data are shown as a continuous line. BCFZ refers to Ballena Celmira Fault Zone, ENFZ to East Nicoya Fault Zone and QSC to Quesada Sharp Contortion.

Acknowledgements

This work was carried out at the Department of Earth Sciences, Seismology Programme, Uppsala University, Sweden. The Swedish Agency for Research Cooperation (SAREC, SERCA project) and the Universidad Nacional de Costa Rica (UNA) provided financial support. Professor S. Horiuchi kindly allowed us to use his computer program for the determination of stress tensors and fault planes from P-wave first motions. Figures were generated using GMT software (Wessel and Smith, 1991, 1995). Suggestions and corrections made by the two reviewers are greatly appreciated.

References

Adamek, S., Tajima, F. and Wien, D.A., 1987, Seismic rupture associated with subduction of the Cocos Ridge, *Tectonics* **6**, 757–774.

Adamek, S., Frolich, C. and Pennington, W.D., 1988, Seismicity of the Caribbean-Nazca boundary: Constraints on microplate tectonic of the Panama region, *J. Geophys. Res.* **93**, 2053–2075.

Cisternas, A., 1985, Esfuerzos y deformaciones en tectónica. In: Udias, A., Muños, D. and Buforn, E. (eds), *Mecanismo de los Terremotos y Tectonica*, Facultad de Ciencias Físicas, Universidad Complutense, Madrid.

Colombo, D., Cimini, G.B. and Franco, R. de, 1997, Three-dimensional velocity structure of the upper mantle beneath Costa Rica from a teleseismic tomography study, *Geophys. J. Int.* **131**, 189–208.

Crosson, R.S., 1976, Crustal structure modeling of earthquake data, 1, Simultaneous least squares estimation of hypocenter and velocity parameter, *J. Geophys. Res.* **81**, 3036–3046.

De Mets, C., Gordon, R.G., Argus, D.F. and Stein, S., 1990, Current plate motions, *Geophysical Journal International* **101**, 425–478.

Dominguez, S., Lallemand, S.E., Malavieille, J. and von Huene, R., 1998, Upper plate deformation associated with seamount subduction, *Tectonophysics* **293**, 207–224.

Escalante, G., 1990, The geology of Southern Central America and Western Colombia. In: G. Dengo and Case, J.E. (eds), *The Geology of North America, The Caribbean Region*, Vol. H., Geological Society of America, Boulder, Colorado, pp. 201–230.

Fan, G., Beck, S.L. and Wallace, T.C., 1993, The Seismic Source Parameters of the 1991 Costa Rica Aftershock Sequence: Evidence for a Transcurrent Plate Boundary, *J. Geophys. Res.* **98**, 15,759–15,778.

Frolich, C. and Apperson, K.D., 1992, Earthquakes focal mechanisms, moment tensors, and the consistency of seismic activity near plate boundaries, *Tectonics* **11** (2), 279–296.

Goes, S.D.B., Velasco, A.A., Schwartz, S.Y. and Lay, T., 1993, The April 22, 1991, Valle de la Estrella, Costa Rica (Mw = 7.7) Earthquake and its Tectonic Implications: A Broadband Seismic Study, *J. of Geophys. Res.* **98** (B5), 8127–8142.

Güendel, F.D. and McNally, K.C., 1982, The Foreshock-Mainshock-Aftershock Sequence of the 1978 (Ms = 7.0) Samara, Costa Rica Earthquake: A Unique Data Set (Abstract), *Earthquake Notes, Seismol. Soc. Am.* **53**, 81.

Güendel, F., McNally, K.C., Lower, J., Protti, M., Saenz, R., Malavassi, E., Barquero, J., Van Der Laat, R., Gonzales, V., Montero, C., Fernandez, E., Rojas, D., Segura, J.D.D., Mata, A. and Solis, Y., 1989, First results from a new seismographic network in Costa Rica, Central America, *Bull. Seismol. Soc. Am.* **79**, 205–210.

Güendel, F., Montero, C., Gonzales, V., Segura, J., Malavassi, E., Fernandez, E., Obaldia, F., Rojas, D., Rodriguez, M., Mata, A., Van Der Laat, R., Barboza, V., Barrantes, O. and Marino, T., 1991, Mainschock-aftershock sequence associated with the Costa Rica earthquake of April 22, 1991, *EOS (American Geophysical Union Transactions)* **72**, 301.

Güendel, F., Pacheco, J. and Protti, M., 1992, The 1990–1991 seismic sequence across central Costa Rica: evidence for the existence of a microplate boundary connecting the Panama Deformed Belt and the Middle America Trench, abstract, *Amer. Geophys. Union, EOS* **73** (43), 399.

Güendel, F. and Protti, M., 1995, The March 7, 1992 Mw = 6.5 Naranjo, Costa Rica earthquake: evidence for segmentation within the subducted Cocos Plate, Abstract XXI General Assembly IUGG, B390.

Hey, R.N., 1977, Tectonic evolution of the Cocos-Nazca spreading center, *Bull. Geol. Soc. Am.* **88**, 1404–1420.

Horiuchi, S., Rocco, G. and Hasegawa, A., 1995, Discrimination of fault planes from auxiliary planes based on simultaneous determination of stress tensor and a large number of fault plane solutions, *J. Geophys. Res.* **100**, 8327–8338.

Isacks, B., and Molnar, P., 1971, Distribution of stresses in the descending lithosphere from a global survey of focal mechanism solution of mantle earthquakes, *Rev. Geophys. Space Phys.* **9**, 103–174.

Kissling, E., Ellsworth, W.L., Ederhart-Phillips, D. and Kradolfer, U., 1994, Initial reference models in local earthquake tomography, *J. Geophys. Res.* **99**, 19635–19646.

Klein, F.W., 1984, User's guide to Hypoinverse, a program for Vax and Pc350 computers to solve for earthquake locations, *U.S. Geological Survey*, Open File Report 84-000.

Kolarsky, R.A., Mann, P. and Montero, W., 1995, Island arc response to shallow subduction of the Cocos Ridge, Costa Rica. In: Mann, P. (ed.), *Geologic and Tectonic Development of the Caribbean Plate Boundary in Southern Central America,* Boulder, Colorado, Geological Society of America, Special Paper, pp. 291–307.

Lay, T. and Wallace, T.C., 1995, *Modern Global Seismology*, Academic Press, San Diego, California, 521 pp.

Mann, P., 1995., Preface. In: Mann, P. (ed.), *Geologic and Tectonic Development of the Caribbean Plate Boundary in Southern Central America,* Boulder, Colorado, Geological Society of America, Special Paper.

Matumoto, T., Ohtake, M., Latham, G. and Umaña, J., 1977, Crustal structure in southern Central America, *Bull. Seismol. Soc. Am.* **67**, 121–134.

Minster, J.B. and Jordan, T.H., 1978, Present-day plate motions, *J. Geophys. Res.* **83**, 5331–5334.

Molnar, P. and Sykes L.R., 1969, Tectonic of the Caribbean and Midle America Regions from focal Mechanisms and Seismicity, *Geol. Soc. Am. Bull.* **80**, 1639–1684.

Nakamura, K., 1977, Volcanoes as Possible Indicators of Tectonic Stress Orientation-Principle and Proposal, *J. Vol. Geotherm. Res.* **2**, 1–16.

Nakamura, K. and Uyeda, S., 1980, Stress Gradient in Arc-Back Arc regions and plate Subduction, *J. Geophys. Res.* **85**, 6419–6428.

Protti, M. and McNally, K., 1990, The March 25, 1990, (ML = 6.8, Ms = 7.0) earthquake sequence at Entrance of the Nicoya Gulf, Costa Rica: a near field study, *EOS AGU Trans.* **71**, 1438.

Protti, M., 1991, *Correlation Between The Age of the Subducting Cocos Plate and the geometry of the Wadati-Benioff Zone Under Nicaragua and Costa Rica*, Master Thesis, University of California, Santa Cruz.

Protti, M., Güendel, F. and McNally, K., 1995, Correlation between the age of the subducting Cocos plate and the geometry of the Wadatti-Benioff zone under Nicaragua and Costa Rica. In: Mann, P. (ed.), *Geologic and Tectonic Development of the Caribbean Plate Boundary in Southern Central America*, Boulder, Colorado, Geological Society of America Special Paper, pp. 309–326.

Protti, M., Schwartz, S.Y. and Zandt, G., 1996, Simultaneous Inversion for Earthquake and Velocity structure Beneath Central Costa Rica, *Bull. Seismol. Soc. Am.* **86**, 19–31.

Quintero, R. and Kulhánek, O., 1998, Pn-Wave Observations in Costa Rica, *Geofisica Internacional* **37**, 171–182.

Schwartz, S.Y., 1995, Source Parameters of Aftershocks of the 1991 Costa Rica and 1992 Cape Mendocino, California, Earthquakes from inversion of Local Amplitude Ratios and Broadband Waveforms, *Bull. Seismol. Soc. Am.* **85**, 1560–1575.

Suetsugu, D., 1995, *Practice on source mechanism*, IISEE lecture Note, IISEE, Buld. Res. Int., Ministry of Construction, Tsukuba, Japan.

Von Huene, R., Bialas, J., Flueh, E., Cropp, B., Csernok, T., Fabel, E., Hoffman, J., Emeis, K., Holler, P., Jeschke, G., Leandro, C.M., Perez Fernandez, I., Chavarria, J.S., Florez, A.H., Escobedo, D.Z., Leon, R., and Barrios, O.L., 1995, Morphotectonics of the Pacific convergent margin of Costa Rica. In: Mann, P. (ed.), *Geologic and Tectonic Development of*

the Caribbean Plate Boundary in Southern Central America, Boulder, Colorado, Geological Society of America, Special Paper, pp. 291–307.

Wessel, P. and Smith, W.H.F., 1991, Free software helps map and display data, *EOS* **72** (441), 445–446.

Wessel, P. and Smith, W.H.F., 1995, New version of the Generic Mapping Tools released, *EOS* **76**, 329.

White, R.A. and Harlow, D.H., 1993, Destructive upper-crustal earthquakes of Central America since 1900. *Bull. Seismol. Soc. Am.* **83**, 1115–1142.

Zoback, M.L., 1992, First- and Second-Order of Stress in the Lithosphere: The world Stress Map Project. *J. Geophys. Res.* **97**, 11703–11728.